A Stand-Alone Surrogate Model for Predicting Protection Heater Delays in Nb_3Sn Accelerator Magnets

Shahriar Bakrani Balani, H. Milanchian, and T. Salmi

***Abstract*—Quench is an irreversible transition where the magnet locally loses its superconducting properties and becomes resistive. Early quench detection and a prompt protection system response are essential to avoid conductor damage. One of the conventional methods for accelerator magnet quench protection is to place resistive heaters on the surface of the coils. The protection heaters are stainless steel strips which are powered with a voltage pulse from capacitor bank discharge. Current is passing through the heaters, generating heat due to the resistivity of the stainless steel. Heat is transferred to the cable by conduction. There is at least one layer of polyimide film and the cable insulation (impregnated glass fiber) between the heater and the superconducting cable. Heater delay is defined as the required time to reach the current sharing temperature in the cable after heater firing. Typically predicting the heater delay requires numerical simulations which are computationally somewhat challenging and require expertise and need of specific software. In this study, we are providing a fast and easily accessible surrogate model for predicting the heater delay in Nb_3Sn magnets. Finite Element Method simulations with COMSOL Multiphysics are used for collecting the dataset and training a supervised artificial neural network algorithm. The model can be used for first estimations of heater delay in Nb_3Sn accelerator magnets during their design phase. In future, the surrogate model could be also integrated with other quench protection design tools to accelerate the detailed protection design of future magnets.**

***Index Terms*—Accelerator magnets, machine learning, neural network, Nb_3Sn dipoles, protection heaters, quench protection.**

I. Introduction

HIGH magnetic field Nb_3Sn dipoles and quadrupoles are currently being developed for the next generation of particle accelerators. Higher magnetic field in dipoles enables the bending of higher-energy particle beams and higher gradient quadrupoles enable stronger focusing of the beam thus leading to increased collision energy and luminosity in experiments [1]. Developing effective quench protection systems is crucial in designing these high-energy density magnets. Quench protection must quickly detect and safely manage quench events, preventing damage to the magnet and surrounding infrastructure due to the violent heating associated with the abrupt loss of superconductivity. Several quench protection methods for low-temperature superconductors (LTS) can be considered, including heater strips [2]. The heater strip technology utilizes trace technology. This involves a thin flexible printed circuit on a polyimide foil with resistive metal heaters made of stainless steel (25 μm thick) which is embedded on the surface of the coil [3]. Protection heaters are fired by capacitor discharge to deliberately initiate a controlled quench across a superconducting magnet. This allows resistive heating in large coil volumes after switching off the magnet current supply and more even distribution of the stored energy in absence of external dump resistor. One of the most important factors influencing the performance of the heaters is the heater delay. It refers to the time interval between the activation of the heater and the moment when it quenches the cable (cable reaches current sharing temperature (T_{cs})) [4]. Consequently, to improve the protection, it is required to reduce the heater delay. Dedicated measurements during magnet tests and numerical simulations can be used to determine the heater delay for different conditions. Salmi et al. [5], [6] developed a computer code called CoHDA (Code for Heater Delay Analysis) for modeling the protection heaters for High-Field (HF) Nb_3Sn accelerator magnets. CoHDA solves a 2D thermal diffusion problem in the cable cross-section (thermal network method) to determine the heat transfer between the heaters and coil. Experimental tests in liquid helium temperatures are naturally more costly compared to the numerical simulation, but they are necessary to validate the numerical models. Baldini et al. [7] studied the influence of heater insulation on the performance of the heater and the durability of the insulation between the heater and coil using destructive tests. Infrared thermal imaging is one of the non-destructive experimental tests for the characterization of heat diffusion in impregnated heaters [8]. Artificial intelligence (AI) techniques [9] have potential to streamline and fasten the design and optimization processes in superconducting magnets [10], [11]. Quench event prediction is one of the most common quench-related properties studies using different AI techniques. Sotnikov et al. [12] developed a machine learning model with the random forest algorithm for the computation of quench behavior in 2G High Temperature Superconductors (HTS). The algorithm is using a Finite Element Method (FEM) model for model training [12]. Other Machine learning algorithms such as Auto-Encoder Deep Neural Networks (AE-DNN)

Received 20 September 2024; revised 26 November 2024 and 5 December 2024; accepted 9 December 2024. Date of publication 30 December 2024; date of current version 10 January 2025. This work was supported in part by the Academy of Finland HiQuench-2-project under Grant 334318 and Grant 336287, and in part by Super20T-project under Grant 324887. *(Corresponding author: Shahriar Bakrani Balani.)*

The authors are with Tampere University, 33720 Tampere, Finland (e-mail: shahriar.bakranibalani@tuni.fi).

Color versions of one or more figures in this article are available at https://doi.org/10.1109/TASC.2024.3523873.

Digital Object Identifier 10.1109/TASC.2024.3523873

[13], k-nearest neighbors (KNN), and Artificial Neural Networks (ANN) [14] methods are used to "predict" the quenches under different magnet conditions.

The numerical simulations of heater delay are experimentally validated [15] but the model development is relatively demanding because the domain includes thin layers of material with very different thermal properties and large temperature gradient. Building or using them requires expertise and suitable numerical codes. In this work we aim to train a neural network surrogate model that is able to predict the heater delay. The model can be easily shared with the community, and it can provide estimations of heater delays without need of complex multiphysics simulation software. Based on our literature AI-based methods has been used in magnet design previously, but there is no machine learning neural model for determination of the heater delay. The neural network model is trained with a dataset from a simplified FEM simulation model, that was previously used in [15]. The remainder of this paper is organized as follows: Section II outlines the parameters influencing the heater delay and creation of the training dataset and libraries used for creating the neural model using machine learning. Section III focuses on the developed machine learning model. Finally, the predicted heater delay from the machine learning model is compared with the heater delay determined by COMSOL numerical simulation and CoHDA code [5].

II. Materials and Methods

The simulated heater delay is defined when the cable reaches the current sharing temperature (T_{cs}). In this study we took the conservative approach to look at the temperature in the center of the cable [16]. Heater related variables include heater thickness (t_h) and heater width (w_h), heater current (I_h), and heater current pulse decay time constant (τ). To reduce the number of the variables; t_h, w_h, and I_h are replaced by heater current density (J_h), and heater thickness is fixed to 0.025 mm. Between the heater and cable there is one layer of Kapton (polyimide film) and one layer of G10. The thickness of Kapton layer is denoted by t_{ka} and thickness of G10 layer is denoted by t_{G10}. The initial temperature of the cable is set at 4.2 K.

The magnet Rutherford cable is composed of Nb_3Sn, Copper, and G10. Based on literature references, thermal properties of each material in the cable such as density (d), specific heat capacity (Cp), and thermal conductivity (K) are considered exogenous parameters. The average thermal properties of the cable are determined according to cable characteristics such as the fraction of copper to Nb_3Sn ($F_{cu/sc}$) in strand and the percentage of G10 in the cable ($\%G10$) and copper residual-resistance ratio (RRR). The magnet operational conditions such as magnet field (B) and magnet current (I_m) influence the thermal properties of the cable components such as thermal conductivity of copper (K_{cu}), specific heat capacity of Nb_3Sn (Cp_{Nb}), and current sharing temperature (T_{cs}). To reduce the number of the input variables of the neural network model, I_m and B are replaced by T_{cs} as an independent variable. The width of the cable (w_{ca}) is another variable influencing the heater delay which is considered as an input variable.

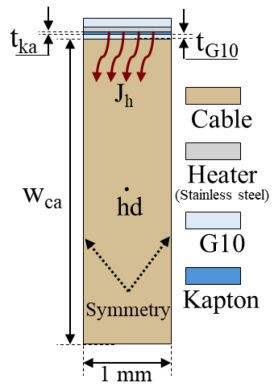

Fig. 1. Illustration of the numerical model adapted to collect the data for the dataset.

TABLE I
Selected Values of the Variables for the Creation of the Dataset

Variable	Selected levels
$F_{cu/SC}$ (1)	0.8, 1.5, 2.2
t_{G10} (mm)	0.1, 0.15, 0.2
t_{ka} (mm)	0.025, 0.05, 0.075
J_h (A.mm^{-2})	200, 333, 466, 600
%G10 (1)	0.1, 0.16, 0.22
τ (ms)	10, 15, 25, 45
w_{ca} (mm)	12.73, 15, 20
B (T)	1, 5, 6, 9, 13, 17
T_{cs} (K)	Based on the critical surface

A. Dataset Creation

The dataset used in this study is generated based on the COMSOL Multiphysics 6.2 model which is validated with experimental data from literature and CoHDA code [15]. A modification has been performed to reduce the computation time The numerical model adapted to create the dataset is presented in Fig. 1. The cable temperature reference point for the current sharing temperature is selected at the center of the cable to be conservative. The simulated heater delays were limited below 50 ms. This means dataset only includes the cases where heater delay is less than 50 ms. The main reason behind this limitation is to facilitate data separation and labeling and reduce the computation time. Additionally, the most important heater design region is for delays shorter than 50 ms. Moreover, we assume that the heating station length is long enough not to influence the delay and neglect its impact. This allows reducing the 2D model to practically 1D simulation.

Before creation of the dataset, a preliminary study was performed to evaluate the influence of each variable on the heater delay. This is required to reduce the number of simulations for the creation of the dataset. Based on the preliminary study, the influence of RRR on the heater delay is negligible. Therefore, it is considered a constant value (150) in all the simulations. As represented in Table I, the 9 most influential variables are selected for the creation of the dataset for the machine learning algorithm. The ranges of the variables were selected based on

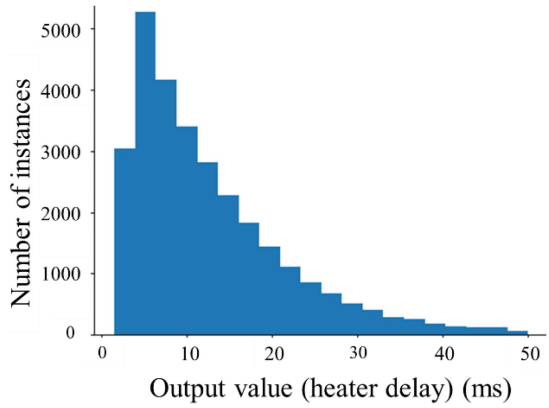

Fig. 2. Distribution of the output values (heater delay) in the dataset.

their typical range in magnet design. For each variable, the upper and lower boundary of the range is selected as a level. A full factorial design of experience (DOE) is performed, in which all the combinations of the variables presented in Table I were simulated. The impact of T_{cs}, was analyzed through data processing on the data exported from the simulations. T_{cs} is selected based on the critical surface and critical temperature (T_c) [17], indicating that the selected T_{cs} value is smaller than T_c in all the cases.

Performing a full factorial DOE increases the accuracy of the model. The heater delay is determined based on the T_{cs} by post-processing the exported data from COMSOL. The average computation time for numerical simulation is approximately 3.5 minutes using a desktop computer with a 12th Gen Intel(R) Core(TM) i7-12700H 2.30 GHz processor. Since the maximum heater delay simulation was set at 50 ms, the cases where the heater delay is above 50 ms are discarded from the dataset. The distribution of the output values (heater delay) in the dataset is demonstrated in Fig. 2. At higher heater delay values the number of observations is reduced. As an example for heater delay between 47.5 ms and 50 ms, less than 200 instances in the dataset are observed, compared to 10000x = ? instances for heater delays between 5 and 20 ms. This could reduce the performance of the neural model at the higher heater delays. On the other hand, most of the observations take place between 2.5 ms and 15 ms, the most critical regime for heater design.

B. Machine Learning

We developed a supervised Deep Neural Network (DNN) machine learning using TensorFlow library to provide a surrogate model for predicting the heater delay. The DNN is created using Keras' Sequential Application Programming Interface (API). Before feeding the data to the model, all the values for the input variables were normalized between 0 and 1. 0 is assigned to the minimum value of the variable in the dataset and 1 is assigned to the maximum value of the same variable. 80% of the data were assigned for training the algorithm and 20% rest was for testing the accuracy of the neural model. The input layer includes 9 variables discussed previously. Two fully connected (dense) layers with 64 neurons and ReLU (Rectified Linear Unit)

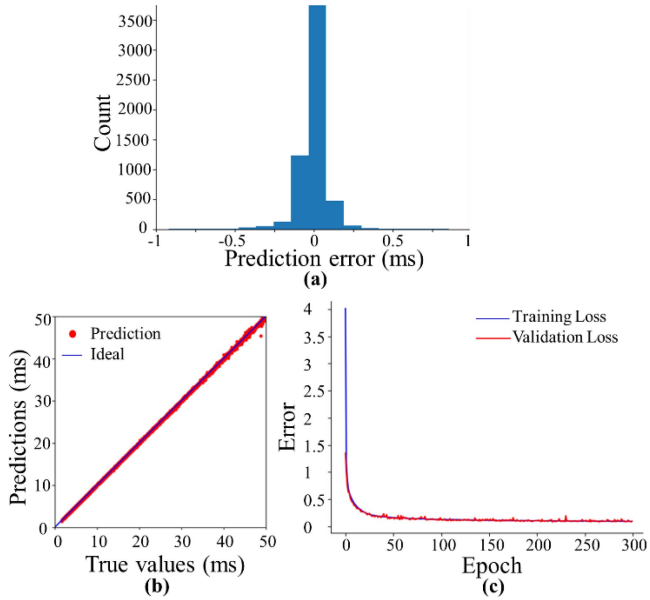

Fig. 3. Performance of the developed model for determination of heater delay; (a) distribution of the neural model error; (b) deviation of true value vs neural model predictions; (c) loss plot of training loss vs validation loss.

activation function are defined. For the output Layer, a fully connected layer with a single neuron is defined. In this layer, no activation function is defined, which means it defaults to a linear activation. This is typical for regression tasks where the output is a continuous value. Adam (Adaptive Moment Estimation) which is a variant of stochastic gradient descent (SGD) is used for the training algorithm. For the compiler, the learning process 'Mean Absolute Error' (MAE) is used as the loss function with a learning rate of 0.001. Three hundred epochs were selected to train the model, meaning that the model will go through the entire training dataset 300 times during the training process.

III. Results and Discussion

A. Model Performance

The performance of the neural network model for heater delay prediction is presented in Fig. 3. The distribution of the neural model errors is illustrated in Fig. 3(a). The neural model values are very close to the values in the training dataset and there is no significant bias. The narrow spread of the prediction error shows the consistency of the neural model. Based on the error distribution histogram, most of the neural values have less than ± 0.5 ms error. The scatter plot for comparison between true values and neural values is illustrated in Fig. 3(b). Red points in the scatter plot represent the neural values, while the diagonal blue line is the ideal line or true value. The cluster of the red points around the line represents the accuracy of the developed neural model. At the higher heater delay (close to 50 ms) the deviation of the neural model results is larger compared to the deviation below 40 ms. The primary reason for the discrepancy near 50 ms is limited number of instances available in the dataset for heater delay in this range. The neural model could also be

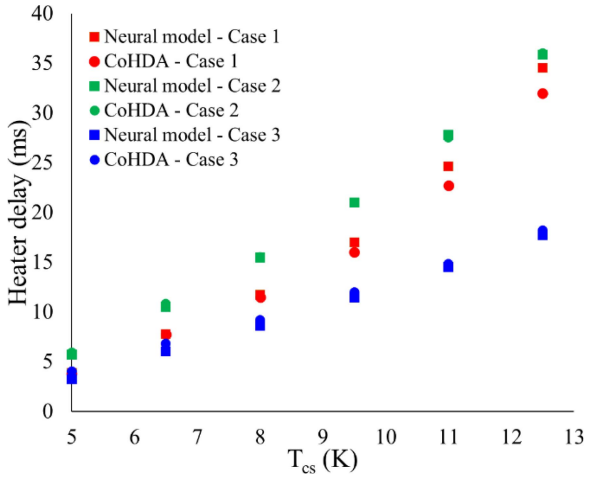

Fig. 4. Comparison between performance of neural model with CoHDA code for three random cases (Case 1 - 3).

used to predict the heater delay above 50 ms. However, the error might be higher comparing the heater delay below 50 ms.

This results in fewer data points available for fitting and consequently, less accuracy of the neural model. The increase of the uncertainties at the higher heater delay is also observed in the literature [16], [18] for real heater design. Consequently, it is crucial to incorporate a sufficient margin in the protection design. The loss plot of the neural model is illustrated in Fig. 3(c). The blue line illustrates the training loss, and the red line is the validation loss. Reducing the training loss curve indicates that the model is learning and improving its performance on the training data by increasing epochs. The validation loss represents the loss calculated on the validation dataset and how well the model generalizes to new data. Decrease and stabilization of the training loss curve and validation loss illustrate the convergence of the model and no overfitting or underfitting is observed. The computation time for heater delay prediction using the neural model is less than 1 s.

The performance of the created neural model has been measured with MAE, Mean Squared Error (MSE), and Root Mean Squared Error (RMSD) methods, see Table III. Low values for all three indexes and their consistency suggest that the neural model performs very well in predicting the heater delay. RMSE is slightly higher than MAE showing that there are some larger errors in the individuals, but they are not substantial.

TABLE II
PERFORMANCE OF THE NEURAL MODEL ACCORDING TO DIFFERENT EVALUATION METRICS

Error Index	Value
Mean Absolute Error (MAE)	0.058 ms
Mean Squared Error (MSE)	0.019 ms^2
Root Mean Squared Error (RMSD)	0.138 ms

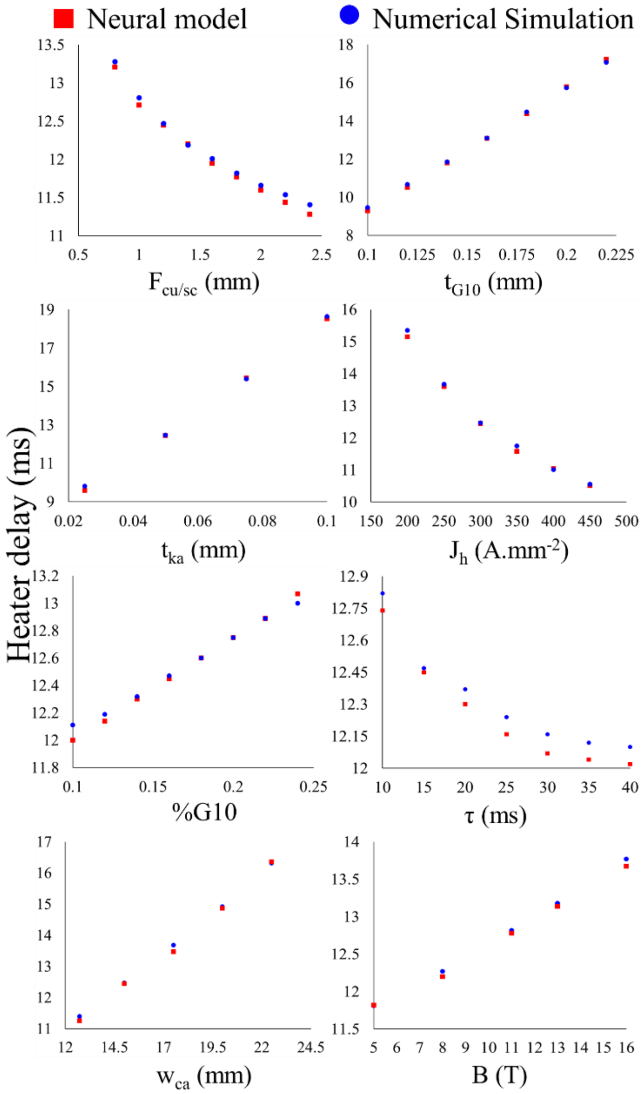

Fig. 5. The comparison between neural model and simulated value (Case 4).

B. Cross-Check Validation

In the previous section, performance of the neural model has been studied on 20% of the instances in the dataset. In this section, the performance of the neural model is investigated through several cross-validations with random cases outside the dataset. The comparison between heater delay determined by the neural model and value from CoHDA is illustrated in Fig. 4. The value of each variable is selected randomly while keeping them different from the levels explained in Table II. The neural values show very good agreement with CoHDA, with an average error of 3-4%. The CoHDA simulation model was adjusted to represent the same geometry (1D) and temperature reference point (center of the cable) as the COMSOL simulation model. The maximum error occurs in case 3 at low T_{cs}, which could be due to the high value selected for τ (48 ms), as it is beyond the range included in the neural network model training dataset. A strong deviation is also observed for case 1 at 13 K. As presented in Fig. 5 increasing the τ value results in an increase in the error of the neural model. The heater delay is very non-linearly dependent on this parameter, which could be the reason for not capturing its impact correctly. The impact of τ saturates at

TABLE III
VALUE OF THE VARIABLES FOR INVESTIGATING THE INFLUENCE OF EACH VARIABLE ON HEATER DELAY

Par.	$F_{cu/SC}$	t_{G10}	t_{ka}	J_h	*%G10*	τ	w_{ca}	B	T_{cs}
Case 1	1	0.12	0.045	250	0.12	20	17	9	*
Case 2	1.2	0.145	0.076	360	0.18	22	18.4	9	*
Case 3	1.8	0.18	0.026	500	0.14	48	14	9	*
Case 4	1.2	0.15	0.05	300	0.16	15	15	8	8

different values depending on the other parameters in the heater simulation case.

C. Sensitivity Analysis

Influence of each variable on the heater delay is determined by the neural model and compared with numerical simulation. In the parametric study shown in Fig. 5, all variables are held constant at their initial values from Case 4 in Table III, except for one variable which is varied in each graph. This analysis allows us to identify which variables are most significant and how they interact with the target.

The comparison between the heater delay determined with the neural model and heater delays derived from the numerical simulation is presented in Fig. 5. The results closely align, demonstrating the model captures the underlying patterns and relationships within the data. The accuracy holds even for input variable values extending beyond the maximum and minimum values outlined in Table I. The impact of *%G10*, τ, B and $F_{cu/sc}$ are narrower compared to other variables which indicates their small influence on the heater delay. However, it is noteworthy that the deviation between the neural model results and numerical simulations increases at higher heater delays. Particularly when these values exceed 40 ms. Fig. 5 demonstrates the linear effect of t_{G10}, t_{ka}, *%G10*, B, and w_{ca} on the heater delay while other variables exhibit a non-linear effect on the heater delay. According to the effect curve of τ in Fig. 5, it reaches a plateau above 30 ms, indicating that beyond this value, τ does not influence the heater delay when the heater current density and other parameters are as in Case 4. The Maximum value of error observed between numerical simulation and neural model value is 2.2% which corresponds to the t_{ka} with 0.025 mm.

D. Neural Network Model Accessibility

After validation of the neural network model, it is saved with the Keras API format for the later use, without the need to re-specify the architecture or retrain the model. Saved model includes model architecture, model weights, optimizer configuration, and training configuration. This model can be downloaded and used as a stand-alone tool to make the prediction. The neural model can be found in public depository (github.com/Shahibak/Heater-delay-prediction-model) [19]. The neural model represents one cable turn in magnet and can be called several times to map the heater delay in different regions of the magnet.

IV. CONCLUSION

We developed and evaluated a stand-alone surrogate model for predicting heater delay in Nb_3Sn accelerator magnet cables. Using a machine learning model offers several key benefits compared to experimental study and numerical simulation. These benefits include speed, cost-effectiveness, and availability for non-expert users. The neural network model was trained with a comprehensive dataset created through numerical simulations with COMSOL Multiphysics software. The Mean Absolute Error (MAE) value of 0.058 ms demonstrates the accuracy of the neural model. The deviation between neural model results and numerical simulations is small, but it increases at higher heater delays. This indicates potential areas for further refinement of the model to enhance its performance in this range. Other future improvement areas are the flexibility to change cable temperature reference point location, more in-depth study of τ and J_h and to include the impact of heater station length.

The computation time of COMSOL simulation was 3.5 minutes, while in the neural model it was 1 second. This reduction in computation time becomes valuable if the model is integrated in real heater design processes or real-time test data analyses which typically involve tens or hundreds of heater delay simulations. Perhaps the biggest advantage here however is that the user does not need to generate the relatively complex numerical model with thin layers and temperature-dependent non-linear material properties but can use this model to quickly estimate the heater delay at various stages of magnet design processes.

REFERENCES

[1] M. Benedikt and F. Zimmermann, "Towards future circular colliders," *J. Korean Phys. Soc.*, vol. 69, no. 6, pp. 893–902, Sep. 2016, doi: 10.3938/jkps.69.893.
[2] L. Coull, D. Hagedorn, V. Remondino, and F. Rodriguez-Mateos, "LHC magnet quench protection system," *IEEE Trans. Magn.*, vol. 30, no. 4, pp. 1742–1745, Jul. 1994, doi: 10.1109/20.305593.
[3] A. Stenvall, T. Salmi, and E. Härö, "Introduction to stability and quench protection," in *Numerical Modeling of Superconducting Applications*, vol. 4, World Sci. Publishing, 2023, pp. 107–185.
[4] S. Feher et al., "Quench protection of SC quadrupole magnets," in *Proc. Part. Accel. Conf.*, Vancouver, BC, Canada, vol. 3, 1997, pp. 3389–3391. doi: 10.1109/PAC.1997.753218.
[5] T. Salmi et al., "A novel computer code for modeling quench protection heaters in high-field Nb_3Sn accelerator magnets," *IEEE Trans. Appl. Supercond.*, vol. 24, no. 4, Aug. 2014, Art. no. 4701810, doi: 10.1109/TASC.2014.2311402.
[6] T. Salmi and A. Stenvall, "Modeling quench protection heater delays in an HTS coil," *IEEE Trans. Appl. Supercond.*, vol. 25, no. 3, Jun. 2015, Art. no. 0500205, doi: 10.1109/TASC.2014.2363523.
[7] M. Baldini et al., "Assessment of MQXF quench heater insulation strength and test of modified design," *IEEE Trans. Appl. Supercond.*, vol. 31, no. 5, Aug. 2021, Art. no. 4701305, doi: 10.1109/TASC.2021.3058223.
[8] M. Marchevsky et al., "Protection heater design validation for the LARP magnets using thermal imaging," *IEEE Trans. Appl. Supercond.*, vol. 26, no. 4, Jun. 2016, Art. no. 4003605, doi: 10.1109/TASC.2016.2530161.
[9] M. Yazdani-Asrami, "Artificial intelligence, machine learning, deep learning, and big data techniques for the advancements of superconducting technology: A road to smarter and intelligent superconductivity," *Supercond. Sci. Technol.*, vol. 36, no. 8, Jul. 2023, Art. no. 084001, doi: 10.1088/1361-6668/ace385.
[10] E. Rivasto, M. Todorović, H. Huhtinen, and P. Paturi, "Optimization of high-temperature superconducting multilayer films using artificial intelligence," *New J. Phys.*, vol. 25, no. 11, Nov. 2023, Art. no. 113046, doi: 10.1088/1367-2630/ad03bb.

[11] D. Wu, D. Sotnikov, G. Gary Wang, E. Coatanea, M. Lyly, and T. Salmi, "A dimension selection-based constrained multi-objective optimization algorithm using a combination of artificial intelligence methods," *J. Mech. Des.*, vol. 145, no. 8, Aug. 2023, Art. no. 081704, doi: 10.1115/1.4062548.

[12] D. Sotnikov, M. Lyly, and T. Salmi, "Prediction of 2G HTS tape quench behavior by random forest model trained on 2-D FEM simulations," *IEEE Trans. Appl. Supercond.*, vol. 33, no. 5, Aug. 2023, Art. no. 6602005, doi: 10.1109/TASC.2023.3262212.

[13] D. Hoang et al., "Intelliquench: An adaptive machine learning system for detection of superconducting magnet quenches," *IEEE Trans. Appl. Supercond.*, vol. 31, no. 5, Aug. 2021, Art. no. 4900805, doi: 10.1109/TASC.2021.3058229.

[14] A. Akbar, N. Riva, and B. Dutoit, "Optical fibre based quench detection in HTS applications using machine learning classifiers," *Physica C, Supercond. Appl.*, vol. 593, Feb. 2022, Art. no. 1354007, doi: 10.1016/j.physc.2021.1354007.

[15] S. Bakrani Balani, T. Salmi, V. Calvelli, H. Felice, and E. Rochepault, "A numerical simulation of quench propagation in Nb_3Sn cables covered with protection heaters," *IEEE Trans. Appl. Supercond.*, vol. 34, no. 5, Aug. 2024, Art. no. 4701205, doi: 10.1109/TASC.2024.3352517.

[16] T. Salmi, G. Chlachidze, M. Marchevsky, H. Bajas, H. Felice, and A. Stenvall, "Analysis of uncertainties in protection heater delay time measurements and simulations in Nb_3Sn high-field accelerator magnets," *IEEE Trans. Appl. Supercond.*, vol. 25, no. 4, Aug. 2015, Art. no. 4004212, doi: 10.1109/TASC.2015.2437332.

[17] L. Bottura and O. Zienkiewicz, "Quench analysis of large superconducting magnets. Part I: Model description," *Cryogenics*, vol. 32, no. 70, pp. 659–667, 1992, doi: 10.1016/0011-2275(92)90299-P.

[18] T. Salmi, T. Tarhasaari, and S. Izquierdo-Bermudez, "A database for storing magnet parameters and analysis of quench test results in HL-LHC Nb_3Sn short model magnets," *IEEE Trans. Appl. Supercond.*, vol. 30, no. 4, Jun. 2020, Art. no. 4703705, doi: 10.1109/TASC.2020.2981304.

[19] S. Bakrani Balani, *Shahibak/Heater-Delay-Prediction-Model*. Sep. 17, 2024, Python. Accessed: Sep. 17, 2024. [Online]. Available: https://github.com/Shahibak/Heater-delay-prediction-model